SARS-CoV-2 cell entry gene ACE2 expression in immune cells that infiltrate the placenta in infection-associated preterm birth

Phetcharawan Lye[1], Caroline E. Dunk[2], Jianhong Zhang[2], Yanxing Wei[2], Jittanan Nakpu[1], Hirotaka Hamada[1], Guinever E Imperio[1,2], Enrrico Bloise[1,3], Stephen G Matthews[1,2,4]**, Stephen J Lye[1,2,4]*,**

[1]Department of Physiology, University of Toronto, Toronto, Ontario, Canada (P Lye, H Hamada, GE Imperio, E Bloise, SG Matthews, SJ Lye).

[2]Lunenfeld-Tanenbaum Research Institute, Sinai Health System, Toronto, Ontario, Canada (J Zhang, Y Wei, J Nakpu, CE Dunk, GE Imperio, SG Matthews, SJ Lye).

[3]Department of Morphology, Federal University of Minas Gerais, Belo Horizonte, Brazil (E Bloise)

[4]Department of Obstetrics and Gynecology and Department of Medicine, University of Toronto, Toronto, Ontario, Canada (SG Matthews, SJ Lye).

*Corresponding author

**Contributed equally

The authors report no competing interests.

Correspondence to:

Stephen Lye, Lunenfeld-Tanenbaum Research Institute, Sinai Health System, Toronto, Ontario, Canada.

Email: lye@lunenfeld.ca

Abstract

COVID-19 infection during pregnancy is associated with an increased incidence of preterm birth but neonatal infection is rare. We assessed pathways by which SARS-CoV-2 could access the placenta and contribute to fetal transmission. Placentas from

pregnancies complicated with chorioamnionitis (ChA), exhibited increased expression of *ACE2* mRNA. Treatment of 2nd trimester placental explants with LPS, induced an acute increase in cytokine expression followed by *ACE2* mRNA. Placental ACE2 protein localized to syncytiotrophoblast, in fetal blood vessels and M1/M2 macrophage and neutrophils within the villous stroma. Increased numbers of M1 macrophage and neutrophils were present in the placenta of ChA pregnancies. Maternal peripheral immune cells (mainly granulocytes and monocytes) express the *ACE2* mRNA and protein. These data suggest that in COVID19 positive pregnancies complicated by ChA, ACE2 positive immune cells have the potential to traffic SARS-CoV-2 virus to the placenta and increase the risk of vertical transmission to the placenta/fetus.

Keywords: SARS-CoV-2, COVID-19, *ACE2*, Chorioamnionitis, Preterm birth, M1, M2 macrophages, Monocyte, Neutrophil, LPS, Placenta

Introduction

A novel coronavirus SARS-CoV-2 (2019-nCoV) appeared in Wuhan, Hubei Province, China on December 30, 2019, and spread rapidly around the world (Schwartz, 2020). The acute respiratory syndrome caused by SARS-CoV-2 was named Corona Virus Disease, COVID-19 by the World Health Organization (WHO). At present there are only a few reports identifying mother to fetus/neonate vertical transmission of COVID-19 infection (Dong *et al.*, 2020). Facchetti et al (2020) recently reported the presence of a placenta intervillous inflammatory infiltrate consisting of neutrophils and monocyte-macrophages expressing activation markers in patients with COVID-19 infection, and

Chen et al (2020) suggested the potential for transmission of SARS-CoV-2 from an infected mother to her fetus/neonate before birth. There is limited data on whether SARS-CoV-2 infections increase the risk of complications in pregnancy (Qiao, 2020). A recent systematic review meta-analysis of 13 publications related to COVID infection in pregnancy from China suggests a high rate of maternal and neonatal complications in infected individuals with a preterm birth rate of 20% and a lower neonatal infection rate of 6% (Capobianco *et al.*, 2020).

The immune system is a core component of the maternal-fetal interface. Disruption of the immune system of a pregnant woman, as in the case of bacterial infection, places the mother and fetus/neonate at risk of other infections, such as viruses, which can impact the course of pregnancy for both mother (e.g. preterm birth) (Silasi *et al.*, 2015) and fetus/neonate (e.g. systemic inflammatory response syndrome) (Francis *et al.*, 2019). Additionally, it has been suggested that viral infection of the placenta modifies the immune response to bacterial products by destroying the normal 'tolerance' to LPS and aggravates the inflammatory response, which in turn leads to preterm labor (Cardenas *et al.*, 2011; Kwon *et al.*, 2014). Immune cells at the maternal-fetal interface play a critical role in a successful pregnancy. In the first trimester they contribute to remodelling of the uteroplacental circulation (Hazan 2010; Smith 2009), and at term an influx of maternal peripheral monocytes into the decidua and myometrium leads to their differentiation into macrophage which generate inflammatory mediators that contribute to the initiation of labour (Hamilton *et al.*, 2012; Shynlova *et al.*, 2020). However, these cells also contribute to pathologies of pregnancy. For example, in cases of acute chorioamnionitis bacterial infection of the fetal membranes and/or placenta results in an increased influx of maternal

73 neutrophils and monocytes into these tissues where the latter differentiate into classical
74 activated inflammatory macrophage (Kim *et al.*, 2015; Cappelletti *et al.*, 2020). The
75 potential adverse consequences to the fetus of placental infection and sensitization to
76 maternal-fetal viral transmission and the mechanisms by which this might occur require
77 further investigation.

78 SARS-CoV-2 cell entry is mediated through angiotensin-converting enzyme 2
79 (*ACE2*), a protease responsible for the conversion of Angiotensin 1-8 (Ang II) to
80 Angiotensin 1-7 (Ang 1-7) (Vickers *et al.*, 2002; Jia *et al.*, 2005). Interactions were
81 identified between the SARS-CoV spike protein and its host receptor ACE2, which
82 regulate both the cross-species and human-to-human transmission of SARS-CoV (Wan
83 *et al.*, 2020), and SARS-CoV-2, and share the same receptor, ACE2 (Zhang *et al.*,
84 2020a). The SARS-CoV spike protein is known to bind ACE2 on the surface of the host
85 cell via its subunit S1, and then fuse to viral and host membranes through subunit S2.
86 Viral attachment is facilitated by two domains in subunit S1, which are from different
87 coronaviruses (Li, 2016). It is currently unknown if SARS-CoV-2 binds in this same
88 fashion. The expression and distribution of ACE2 has been reported in human fetal heart,
89 kidneys, liver, lung, and placenta (Crackower *et al.*, 2002; Hamming *et al.*, 2004; Pringle
90 *et al.*, 2011a). *ACE2* mRNA expression has also been found in early gestation placenta
91 (Pringle *et al.*, 2011a; Bloise *et al.*, 2020). In addition, ACE2 protein levels were found to
92 be abundant in the syncytiotrophoblast layer (STB) and villous stroma, while less intense
93 in the trophoblast layer (CTB) (Pringle *et al.*, 2011a). The STB provides the interface
94 between the maternal blood, containing immune cells, and the extraembryonic tissues
95 and fetus (Knöfler *et al.*, 2019; Facchetti *et al.*, 2020). Interestingly activated

96 macrophages in patients with heart failure have been shown to express high levels of the
97 SARS-CoV-2 receptor, *ACE2* (Keidar *et al.*, 2005). Furthermore, in patients with chronic
98 obstructive pulmonary disease (COPD) activation of neutrophils, NK cells, Th17 cells,
99 Th2 cells, Th1 cells, dendritic cells, and TNFα secreting cells can be induced by
100 overexpression of ACE2 leading to a severe inflammatory response (Li *et al.*, 2020a).
101 Since these immune cells can potentially engage the SARS-CoV-2 virus, they may also
102 represent a reservoir for the virus and a vector for the virus to infect the placenta/fetal
103 membranes in cases of chorioamnionitis.

104 We hypothesize that the presence of an intrauterine bacterial infection will activate
105 peripheral maternal macrophage and neutrophils and cause them to target the uterus and
106 intrauterine tissues. If these immune cells express the SARS-CoV-2 cell entry protein,
107 ACE2, then these cells have the potential to transport virus to the placenta and thereby
108 increase the risk of placental infection and vertical transmission of the virus to the fetus.

109

110 **Results**

111 **Chorioamnionitis and LPS exposure are associated with increased placental *ACE2***
112 **expression and an inflammatory cytokine/chemokine response.**

113 Placental *ACE2* mRNA expression was significantly increased ($P<0.01$) in pregnancies
114 complicated with PTB in the presence of ChA compared with PTB alone or with
115 uncomplicated spontaneous vaginal delivery (SVD) or not in labour (elective caesarean
116 section, ELCS) term pregnancies (Figure 1A). Placental mRNA expression of *CCL2* was

117 also significantly increased in ChA (P<0.05) compared to all other groups but there was

118 no significant increase in *IL6/8* mRNA expression (Figure 1C-D).

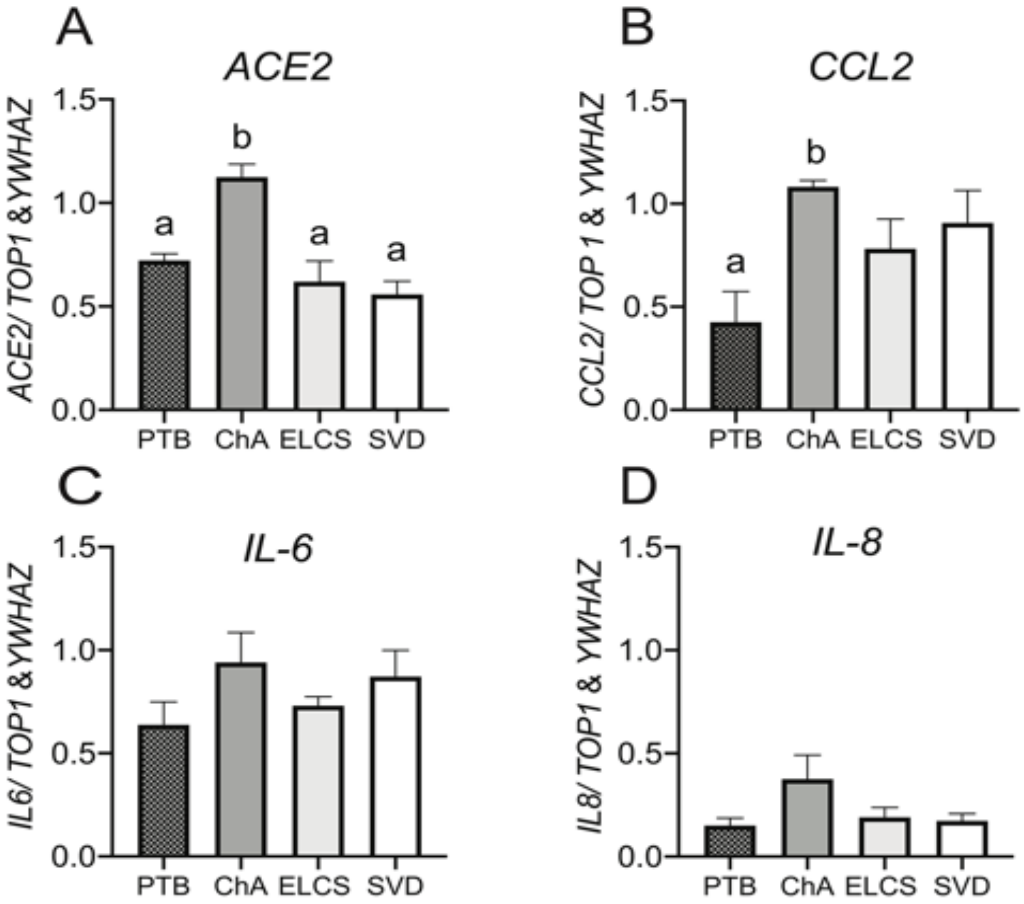

119

120 **Figure 1. *ACE*, and chemokine mRNA expression is increased in placenta from preterm labor with**
121 **chorioamnionitis (ChA).** Bar charts show the relative levels of *ACE2* **(A)**, *CCL2* **(B)**, *IL-6* **(C)**, and *IL-8* **(D)**
122 mRNA in placentas from PTB, ChA, SVD and ELCS deliveries, assessed by real time qPCR. Data are
123 normalized by the geometric mean of *TOP1* and *YWHAZ* (reference genes), N=6-7/group. Statistical
124 differences were tested by Tukey's multiple comparisons test. Data are presented as mean ± SEM. Different
125 letters indicate a difference between groups of p<0.05.

126 Treatment of 2nd trimester placental explants with LPS (10 μg/mL) from elective

127 terminations of healthy normal pregnancies resulted in a rapid (4 hour) significant

128 increase in placental expression of cytokine (*IL-6/8* and *TNFα* mRNA; *P*<0.05) (Figure
129 2D-E), as well as higher (but non-significant expression of the chemokine *CCL2* (P=0.06))
130 (Figure 2B). Cytokine/chemokine expression returned to basal levels 24 hours post-LPS
131 treatment, at which time expression of *ACE2* mRNA in the placental explants increased
132 significantly (p<0.05) (Figure 2A).

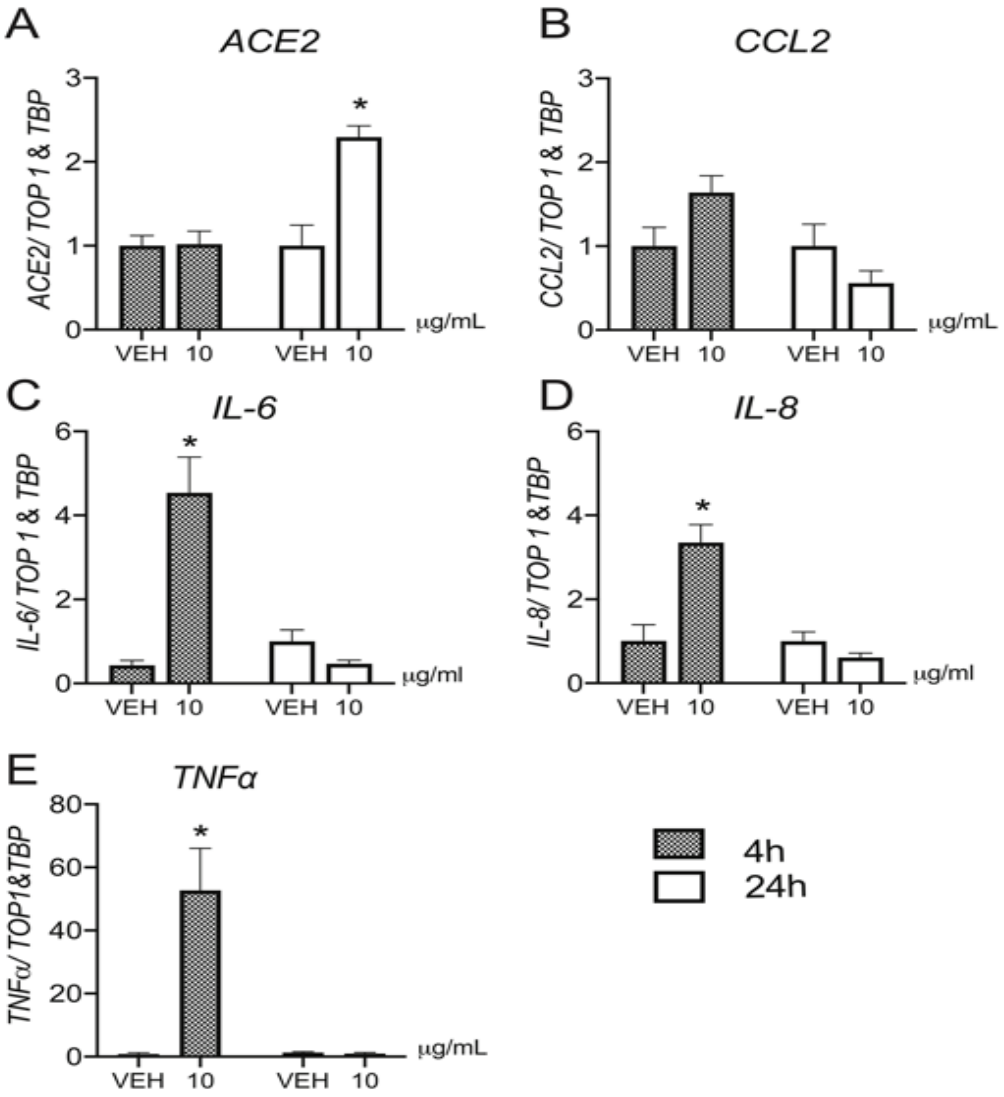

133

134 **Figure 2. Effect of LPS on *ACE2*, *CCL2*, *IL-6/8* and *TNFα* mRNA expression in second trimester**
135 **human placental explants.** Second trimester placental explants were treated with LPS (10 μg/mL), or
136 vehicle for 4 and 24 hours and mRNA levels of *ACE2* **(A)**, *CCL2* **(B)**, *IL-6* **(C)**, *IL-8* **(D)** and *TNFα* **(E)**, were
137 quantified by qPCR (n=5/group). Data are normalized by the geometric mean of *TOP1* and *TBP* (reference
138 genes). Data are expressed as means ± SEM. Statistical differences were tested using a paired *t*-test.
139 *p<0.05, versus vehicle.

140 In contrast to the elevated expression of *ACE2* mRNA, we did not detect any increase in
141 ACE2 protein within the placentas of preterm pregnancies associated with ChA, although
142 the levels of ACE2 protein in preterm placentas (with or without ChA) were significantly
143 higher (p<0.05) than in placentas at term in the presence or absence of labour (Figure
144 3B).

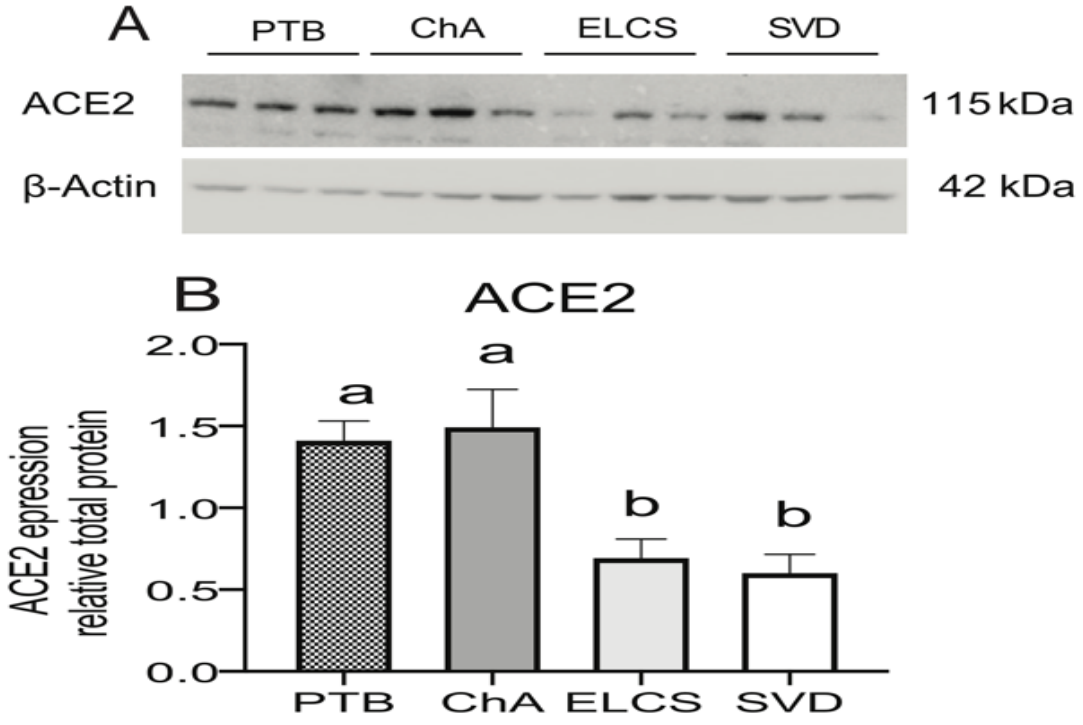

145

146 **Figure 3. Placental ACE2 protein levels are increased in PTB with/without chorioamnionitis (ChA)**
147 **as compared to term.** Protein lysates of placentas from PTB, ChA, ELCS and SVD deliveries were
148 assessed for level of ACE2 protein by western blotting. **(A)** Representative western blot images and **(B)**
149 densitometric analysis of ACE2 protein level, normalized by *β*-actin (loading control for protein), N =
150 6/group. Statistical differences were tested by Tukey's multiple comparisons test. Data are presented as
151 mean ± SEM. Different letters if $p<0.05$.

152 Since ACE2 total protein was not increased in ChA placentas, we next determined the
153 localization of ACE2 protein in the placentas from complicated and uncomplicated
154 pregnancies. This analysis revealed expression of ACE2 in the syncytiotrophoblast
155 (STB), which is the fetal tissue in direct connection with maternal blood and in the fetal
156 blood vessels within the placental villous core. We also observed the presence of ACE2
157 immunoreactivity in histologically-identified macrophages within the placental villous
158 stroma and in association with perivascular cells surrounding the fetal blood vessels and
159 in some fetal blood cells (Figure 4A). ACE2 expression was also present in extravillous
160 trophoblast (EVT) (Figure 4B) and in decidual stromal cells within the placental basal plate
161 (Figure 4C), as well as immune cells within maternal blood present in the intervillous
162 space (Figure 4D).

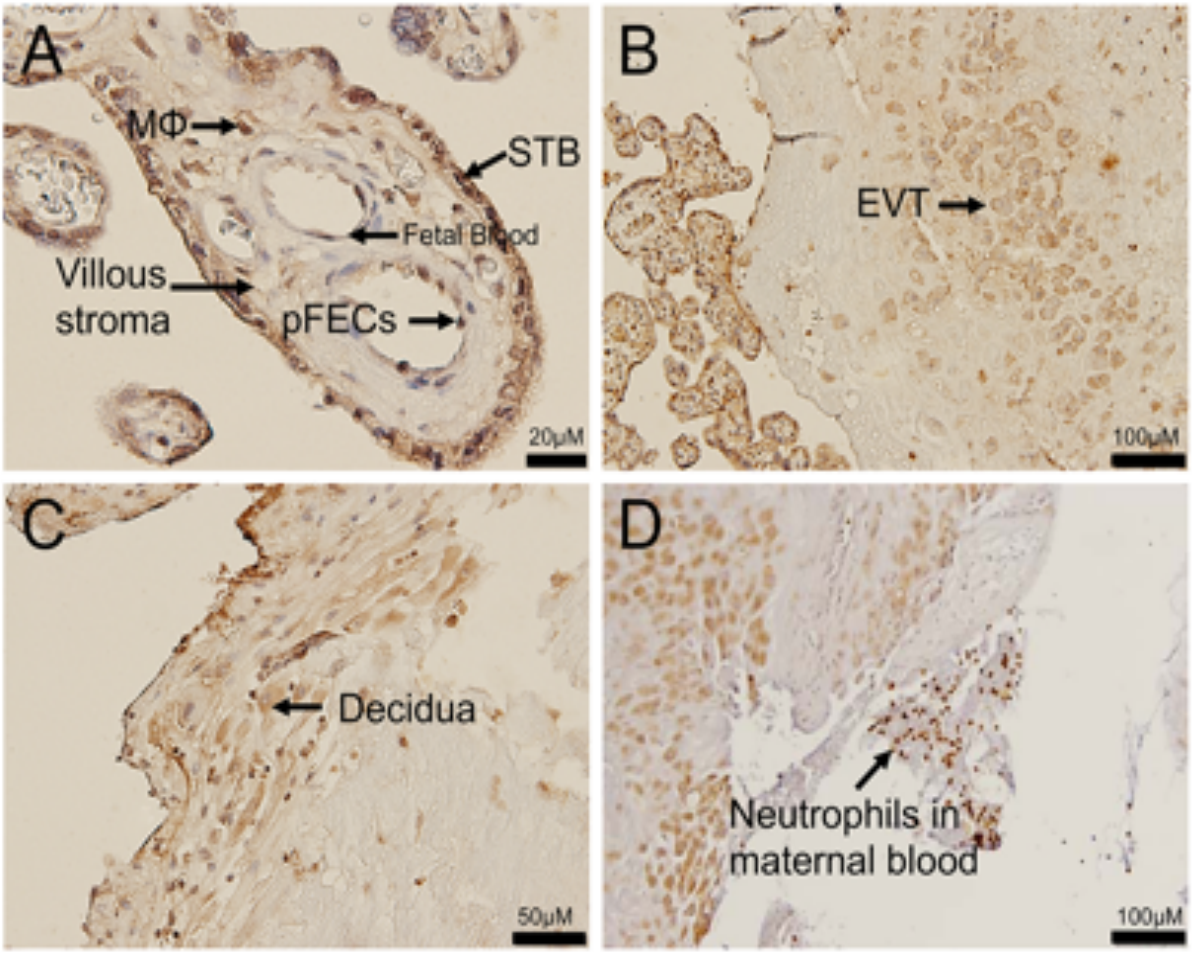

Figure 4. ACE2 localization in the placenta and in maternal intervillous immune cells. Representative images of ACE2 immunostaining in a placenta from an uncomplicated PTB delivery (**A)** ACE2 staining was localized predominantly in the syncytiotrophoblast layer (STB), fetal blood vessel (pFECs) and fetal hoefbauer cells (MΦ) of the placental villi. (**B)** ACE2 also localised to extravillous trophoblast (EVT) within the basal plate of the placenta and in **(C)** decidual stromal cells. **(D)** ACE2 expression in maternal neutrophils of maternal blood clot adjacent to the decidua, Sections were counter-stained with hematoxylin. N=6/group. Scale bar represents 100μm.

The finding of ACE2 expression in histologically-identified immune cells within the placenta led us to undertake further characterization of these cells in placentas from pregnancies complicated by PTB, in the presence or absence of ChA, as well as term pregnancies with and without the onset of labour. We used monoclonal antibodies specific

175 for CD68 (which detect the macrophage population); MHC-II - a marker of M1
176 macrophage; CD206 - a marker of M2 macrophage; and neutrophil elastase (NE) - a
177 marker of neutrophils. Representative images of immunohistochemical staining revealed
178 expression of ACE2 was localized to syncytiotrophoblast of all pregnancy groups (Figure
179 5 A-D) with a reduced intensity of staining in term groups than in preterm groups. ACE2
180 staining was also apparent in stromal cells which resembled macrophage and neutrophils
181 (shown in Figure 5 E-T). Staining with CD68 revealed the presence of macrophage within
182 the placental villous of all pregnancy groups (Figure 5 E-H) and further analysis identified
183 these to be both M1 (inflammatory) and M2 (angiogenic) sub-types. (Figure 5 I-P). The
184 M1 macrophage were present throughout the stroma as well as being associated with
185 fetal blood vessels. Staining with NE detected the presence of neutrophils within the
186 placental vasculature and villi of all pregnancy groups (Figure 5 Q-T). The distribution of
187 these immune cells did not appear to be equal across the patient groups, therefore we
188 sought to quantify their number using Image analysis. Total macrophage numbers were
189 similar in ChA and PTB control groups however, both of these groups had higher numbers
190 of macrophage than the term groups (SVD, ELCS; ($p<0.01$) (Figure 5U). In contrast, the
191 number of M1 macrophages was significantly increased ($p<0.001$) in ChA patients
192 compared to PTB, SVD and ELCS groups (Figure 5V). Whereas, the number of M2 was
193 significantly higher ($p<0.001$) in PTB patients compared to ChA, SVD and ELCS groups
194 (Figure 5W). Quantification of neutrophil numbers across patient groups revealed
195 significantly higher numbers in ChA pregnancies than in the PTB, SVD or ELCS groups
196 (Figure 5X; $p<0.001$).

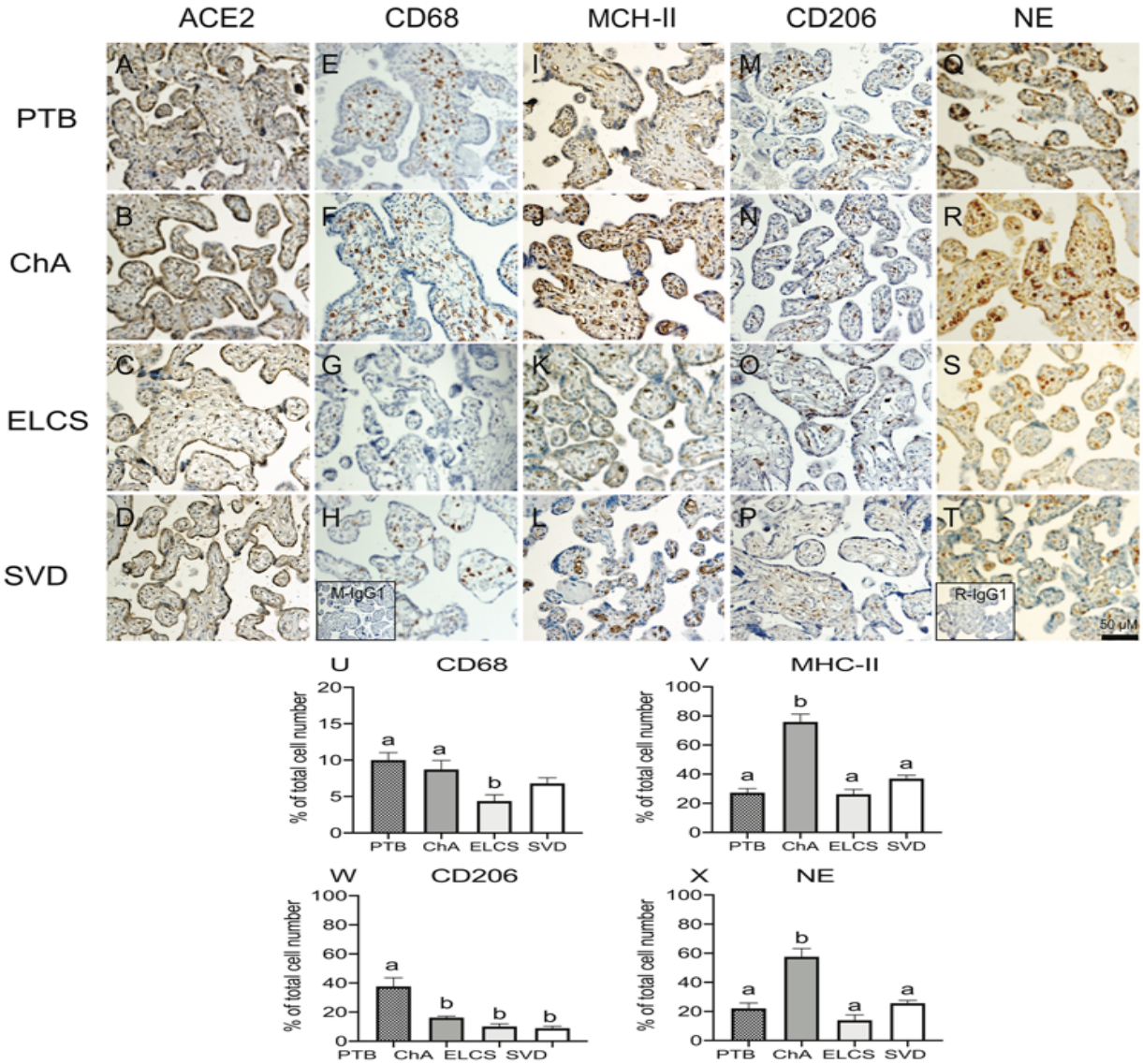

197

198 **Figure 5. Localization and quantitation of placental ACE2, CD68 (macrophage marker), MHC-II (M1**
199 **marker), CD206 (M2 marker) and neutrophil (NE) staining in complicated and uncomplicated**
200 **pregnancies.** Representative images of ACE2 **(A-D),** M1 **(MHCII E-H)**, M2 **(CD206 I-L)**, CD68 **(M-P)**, and
201 NE **(Q-T)** staining in preterm and term placentas (N=6 in each group). Inserts (bottom left) in H mouse IgG1
202 and T rabbit IgG1 isotype control staining. Scale bar represents 50µm. Image analysis quantitation of
203 positively stained immune cells as a proportion of the total cells number was performed on a randomly
204 selected 5% of the total tissue area of each placental section. (**U)** CD68 (**V)** M1 **(W)** M2 **(X)** NE. Statistical

205 differences were tested by Tukey's multiple comparisons test. Data are presented as mean ± SEM. Different
206 letters represent values significantly $p<0.05$.

207 Next we determined whether ACE2 is localized within infiltrated immune cell populations
208 in the ChA placenta, by undertaking co-localization immunofluorescence analysis of
209 ACE2 and CD68 (macrophage), MHC-II (M1), CD206 (M2) and NE (neutrophil) markers.
210 Co-localization of ACE2 in macrophages (M1 and M2) and neutrophil was detected,
211 confirming our previous histological findings that infiltrated macrophages within the
212 placenta express ACE2 and also identifying infiltrating placental neutrophils as
213 expressing ACE2. Immune cells expressing ACE2 were localized in the villous stroma
214 and adjacent to fetal blood vessels. Only a subset of each of immune cells expressed
215 ACE2 (Figure 6 A-L).

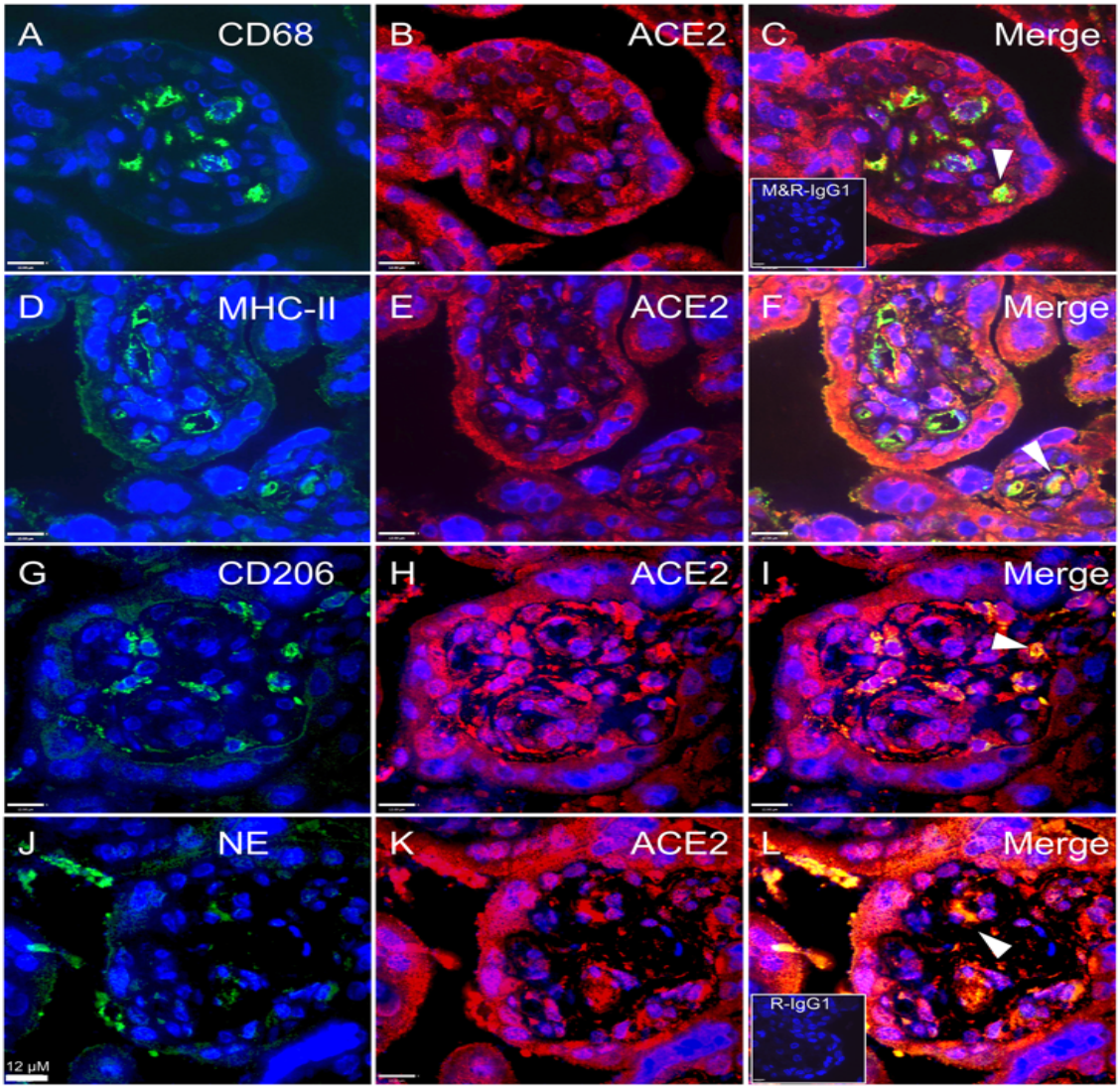

Figure 6. Co-localization of SARS-CoV-2 associated cell-entry protein, ACE2, within specific immune cell populations in ChA placenta. Representative images of ACE2, CD68, M1, M2 and NE staining in immunofluorescence (ACE2; red color and M1, M2, macrophage and NE; green color), macrophage co-staining with ACE2 **(A-C**) M1 co-staining with ACE2 **(D-F)**, M2 co-staining with ACE2 **(G-I)** and neutrophil co-staining with ACE2 **(J-L)**. Co-localization of ACE2 and markers of macrophage and neutrophil confirmed the ACE2 localization within placental macrophages and neutrophils. ACE2 expressing immune cells were present in the villous stroma and adjacent to fetal blood vessels. Only a subset of each of immune cells expressed ACE2. Arrows show ACE2 staining within CD68, M1, M2 and NE stained cells. Sections were counter-stained with DAPI (blue color) or co-staining (yellow color). Inserts (bottom left) in **(C)** mouse and rabbit IgG1 isotype control and **(L)** rabbit IgG1 isotype control staining. N=3/group. Scale bar represents 12 µm.

228 **Expression of *ACE2*/ACE2 in circulating maternal immune cells.**

229 Expression of *ACE2* mRNA was detected in circulating granulocytes, monocytes and
230 lymphocytes from pregnant women, though levels were quite variable and were not
231 significantly different across cell types (Figure 7A). Flow cytometry also revealed that
232 ACE2 was expressed in fractions of circulating granulocytes, monocytes and neutrophils.
233 A greater fraction of circulating granulocytes were found to be positive for ACE2 than
234 lymphocytes, but not monocytes ($p<0.05$; Figure 7B).

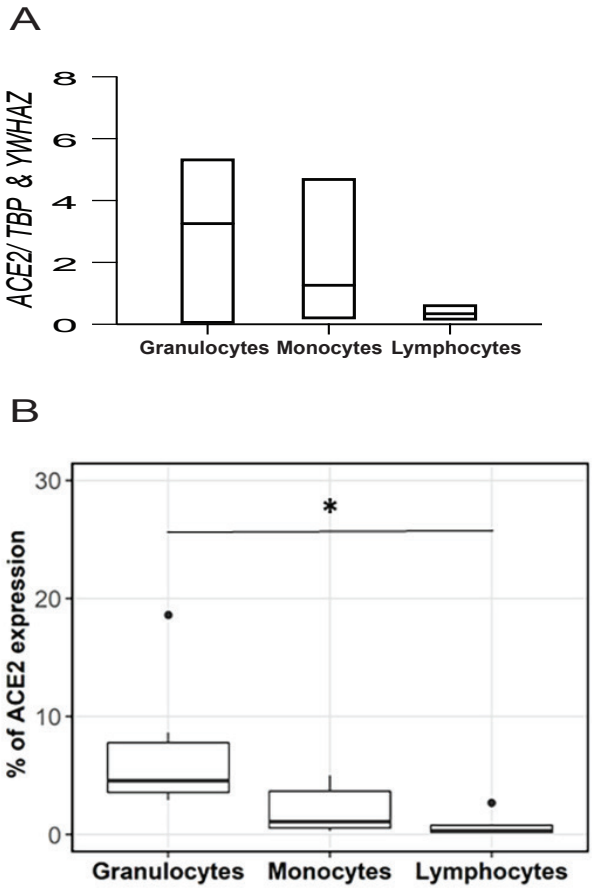

235

236 **Figure 7. The surface expression of ACE2/*ACE2* on circulating granulocytes, monocytes and**
237 **lymphocytes in pregnant women.**
238 **(A)** The relative expression of *ACE2* mRNA on granulocytes, monocytes and lymphocytes in maternal
239 peripheral blood. There are no different between all of group (N=4/group). Statistical differences were tested

240 by Tukey's multiple comparisons test. Data are presented as mean ± SEM. **(B)** Peripheral human blood
241 cells were stained with anti-human ACE2 and CD45 antibodies. The percentage of ACE2+ cells was
242 calculated according to the gating of viable CD45+ granulocytes, monocytes and lymphocytes. Statistical
243 analyses were performed by R software (3.4.3). Multiple comparisons were conducted by Kruskal-Wallis
244 test and Wilcoxon test was followed to examine the statistical difference between two groups. N=6/group.
245 *, $p < 0.05$.
246

247 **Discussion**

248 In this study we provide evidence that under conditions of intrauterine
249 infection/inflammation there is an influx of ACE2 expressing neutrophils and macrophage
250 into the placenta. We suggest that this is a potential mechanism by which maternal-fetal
251 vertical transmission could occur in COVID 19 infected pregnancies.

252 We first demonstrated that *ACE2* mRNA levels were increased in the placenta of
253 pregnancies complicated by chorioamnionitis compared to placentas from patients of
254 similar gestational age with no evidence of infection, or from term pregnancies (collected
255 from non-laboring or laboring deliveries). Despite this increase in mRNA, the expression
256 of ACE2 total protein levels (measured by WB) was not different in the placenta from
257 patients with PTB and chorioamnionitis compared to those from PTB without
258 chorioamnionitis, although both preterm groups expressed higher levels of ACE2 than
259 placentas from patients at term, in the presence or absence of labour. Previously, it has
260 been reported that there is minimal expression of ACE2 mRNA in the placenta throughout
261 pregnancy (Pringle *et al.*, 2011b; Bloise *et al.*, 2020; Li *et al.*, 2020b). However, we
262 recently demonstrated that placental expression of *ACE2* mRNA is gestational-age
263 dependent with the highest levels in early pregnancy and low to undetectable levels

264 towards term (Bloise *et al.*, 2020). Our current data suggest a similar gestational-age
265 dependence pattern for ACE2 protein.

266 We found differences in the cellular distribution of ACE2 in the placenta of patients
267 with ChA. Immunohistochemical analysis localized ACE2 to the STB layer, which is
268 exposed to the maternal circulation as well as in the vascular endothelium of the fetal
269 circulation. Staining was also present in extravillous trophoblast (EVT), and decidual
270 stromal cells. Our findings are consistent with other studies that ACE2 is highly expressed
271 in cells at the maternal-fetal interface including, STB, endothelial and perivascular cells
272 and EVT (Valdés *et al.*, 2006). Acute chorioamnionitis refers to the presence of intra-
273 amniotic infection or "amniotic fluid infection syndrome" (Romero *et al.*, 1992; Kim *et al.*,
274 2015). Acute chorioamnionitis can also occur in the absence of demonstrable
275 microorganisms with "sterile intra-amniotic inflammation", and is induced by "danger
276 signals" or DAMPs released under conditions of cellular stress, injury or death (Romero
277 *et al.*, 1992; Gomez-Lopez *et al.*, 2019). The characteristic histologic and defining
278 features of acute chorioamnionitis is a diffuse infiltration of neutrophils into the fetal
279 membranes (Redline *et al.*, 2003; Kim *et al.*, 2015). All of the placentas in the ChA group
280 were confirmed, by a placental pathologist, to be Grade 1/2, stage 2/3 with fetal
281 inflammation of the membranes (amnion and chorion) and umbilical cord (Table 1).
282 Importantly, we noted expression of ACE2 in immune cells within the ChA placenta.
283 These cells were characterized to be predominantly M1 macrophage and neutrophils,
284 many of which were found in close association or within the wall of fetal blood vessels.
285 Quantification of the number of these cells in the placenta from all patient groups
286 revealed, as expected, significantly greater numbers of these immune cells in

287 pregnancies complicated by acute stage 2/3 ChA than the other pregnancy groups. A
288 recent study has shown that both maternal and fetal neutrophils are present in the
289 amnionitic fluid of women with a confirmed intraamniotic infection and/or inflammation
290 (Gomez-Lopez *et al.*, 2017). We did not confirm that the immune cells within the placental
291 villi were of maternal or fetal origin in this study. However, we did also observe a maternal
292 intervillous infiltrate of ACE2 expressing maternal neutrophils and macrophage in the ChA
293 placenta. Further, mRNA and flow cytometric analysis of ACE2 expression by specific
294 immune subsets in maternal peripheral blood revealed expression of the SARS CoV-2
295 cell entry protein in neutrophils, monocytes and lymphocytes, with the fractions of
296 neutrophils expressing ACE2 being significantly higher than in lymphocytes, but not
297 monocytes. The surface expression of ACE2 on these peripheral immune cells, provides
298 a route by which the virus could enter these cells in the peripheral circulation. Since
299 intrauterine infection (as in the case of chorioamnionitis) leads to activation and targeting
300 of maternal immune cells (particularly neutrophils and monocytes) to the placenta
301 (Glauser *et al.*, 1991; Liu *et al.*, 2018), this would provide a direct path which might
302 facilitate the transmission of viral particles into the placental bed, and subsequently to the
303 fetus. Thus, maternal immune cells could act as the vector for SARS CoV-2 to infect the
304 placenta and or fetus.

305 Our data showing that LPS treatment (a model of bacterial infection and
306 chorioamnionitis) of second trimester placental explants induces a rapid induction of
307 chemokine/cytokines (*CCL2, IL-6/8* and *TNF*α) transcripts and *ACE2* mRNA at 24 hours
308 provides support that placental bacterial infection might increase the opportunity for
309 placental infection by SARS CoV-2. Since syncytiotrophoblast and placental resident

310 immune cells express ACE2 two potential routes for viral infection might exist, one
311 through direct interaction between virus and the outer (syncytial) surface of the placenta
312 and one through the influx of virus containing immune cells. Moreover, since the activated
313 immune cells infiltrating into the placenta can release proinflammatory cytokines this
314 might further enhance placenta *ACE2* mRNA expression (Liu *et al.*, 2018). Whether
315 bacterial LPS can sensitize the placenta to infections by SARS-CoV-2 is not known, and
316 requires further study.

317 There is conflicting data as to whether SARS-CoV-2 can be transmitted to the fetus
318 through the placenta in women with COVID-19. Early reports of obstetric and neonatal
319 outcomes of pregnant women from China with COVID-19 suggested that SARS-CoV-2
320 infection in pregnancy results in limited neonatal infection (Rasmussen *et al.*, 2020; Zhang
321 *et al.*, 2020b). However, an increasing number of studies reporting neonatal cases with
322 congenital or intrapartum infection. So far, 10 infants with SARS-CoV-2 infection meet
323 these criteria based on a classification system defined by Shah et al. (Shah *et al.*, 2020)**.**
324 Notably, a clinical case report revealed that a neonate born to a COVID-19 infected
325 pregnant woman was tested positive for SARS-CoV-2 after 36 hours of postnatal life
326 (Wang *et al.*, 2020), which meets the criteria of intrauterine transmission (Blumberg *et al.*,
327 2020). In addition, in one preterm pregnancy case, the baby tested negative for COVID-
328 19 at birth, and positive 24 hours later (Zamaniyan *et al.*, 2020). Three other neonates
329 showed increased immunoglobulin M (IgM) antibodies specific to COVID19 at birth (Zeng
330 *et al.*, 2020). There is also a growing body of evidence demonstrating infection of the
331 placental membrane and the villous trophoblasts, a recent electron microscopy study has
332 demonstrated the presence of SARS-CoV-2 in placental STB (Algarroba *et al.*, 2020) and

333 Baud et al have reported a case of SARS-CoV-2 positivity in the placental submembranes
334 and cotyledons together with mixed inflammatory infiltration and funicity in pregnant
335 woman in the second trimester (Baud *et al.*, 2020). In this case, placental infection of
336 SARS-CoV-2 was confirmed by the virologic findings from specimen obtaining from the
337 fetal surface. Previously, various pathways of viral transplacental migration were
338 concluded based on the studies of Zika virus, including transmission from maternal blood
339 to EVT, transcytosis via syncytiotrophoblast-expressed receptors, or spreading by
340 infected maternal immune cells (Chen *et al.*, 2020; Karimi-Zarchi *et al.*, 2020).These data
341 support our hypothesis of an increased risk of placental and fetal transmission of SARS-
342 CoV-2 in cases of intrauterine infection/inflammation and chorioamnionitis.

343 In conclusion, our data show that the presence of an intrauterine bacterial infection
344 results in the infiltration of ACE2 expressing maternal macrophage and neutrophils into
345 and across the placental tissues (Figure 8). These ACE2 expressing immune cells have
346 the potential to transport virus to the placenta in cases of COVID-19 infection in pregnancy
347 and increase the risk of placental infection and vertical transmission of the virus to the
348 fetus.

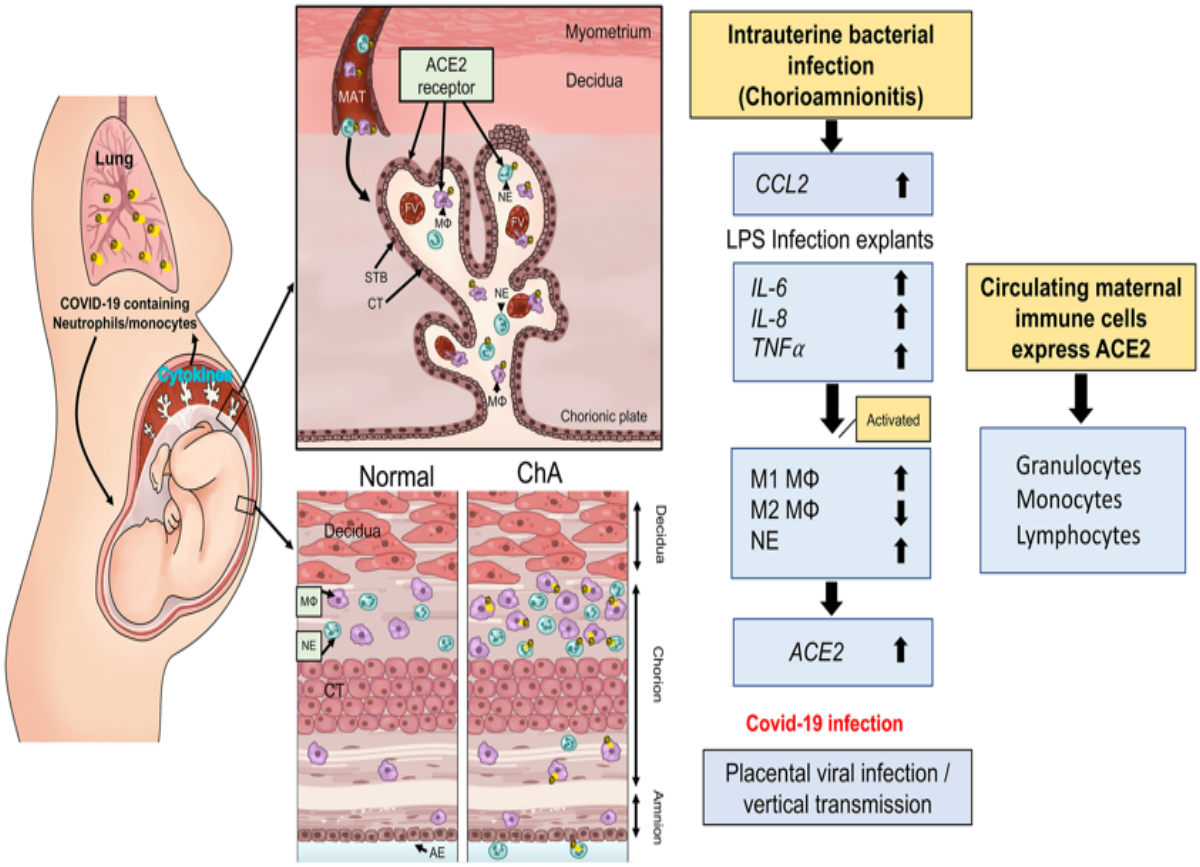

Figure 8. Schematic model by which maternal immune cells could bring SARS-CoV-2 to the placenta and increase risk of vertical transmission in pregnancies complicated by intrauterine infection. Intrauterine bacterial infection, such as occurs in chorioamnionitis (ChA), leads to increased expression and release of chemokine/cytokines by the placenta that in turn induce activation of maternal immune cells, notably M1 macrophage and neutrophils. These cells then target the sites of infection in the placenta/fetal membranes. Subsets of these immune cells express the SARS-CoV-2 cell entry protein, ACE2, and thus are targets for viral uptake in women infected with SARS-CoV-2. The virus may then be hypothetically transported to the placenta increasing the potential for vertical transmission of the virus to the fetus. MAT= maternal blood, FV= fetal vessel, MΦ= M1 macrophage, NE= neutrophil, STB= syncytiotrophoblast, layer CT= cytrophoblast.

363 **Methods**
364

365 **Ethical Approval**

366 This is a cross-sectional study involving placental tissue collection from pregnancies
367 (25.3-36.0 weeks' gestation) complicated by preterm birth (PTB; N=12) or preterm birth
368 with chorioamnionitis (ChA; N=12) or from term pregnancies (>37 weeks' gestation) from
369 healthy women in labour (vaginal delivery, SVD; n=12) or not in labour (elective
370 caesarean section, ELCS; N=12). Second trimester human placental tissues were
371 collected at 16–20 weeks of pregnancy (N=5/group). All clinical information is depicted in
372 Table 1.

373

374 **Table 1.** Clinical profile of placental tissues. BMI, (Body Mass Index); V, (Vaginal), C,
375 (Caesarean section with no labor); CL, (Caesarean section with labor); S1, (Stage1); S2,
376 (Stage2); S3, (Stage3); Y/N, (Yes/No).

	PTB (N=12)	**ChA** (N=12)	**ELCS** (N=12)	**SVD** (N=12)
Maternal Characteristics				
Maternal Age (years)	29.6 ± 1.83 (21-43)	28.5 ± 2.25 (17-40)	35.8 ± 0.85 (34-42)	32.4 ± 1.06 (27-43)
Labor (Y/N)	10:2	11:1	0:12	12:0
BMI	22.4 ± 1.18 (18.26-29.75)	23.8 ± 1.12 (18.30-29.75)	22.6 ± 1.77 (15.24-32.44)	23.2 ± 1.34 (19.08-32.91)
Fetal Characteristics				
Gestational age (weeks)	31.7 ± 0.93 (25.3-36.0)	29.3 ± 1.01 (26-33)	38.6 ± 0.30 (37-41)	39.0 ± 0.32 (37-40.4)
Mode of Delivery (V:C:CL)	2:1:9	5:1:6	0:12:0	12:0:0
Neonatal sex (Male/ Female)	9:3	8:4	6:6	7:5
Pathology Characteristics				
Chorioamnionitis (S1, S2, S3)	No	1:10:1	No	No
Glucocorticoids treatment	Yes	Yes	No	No

377

378 Human peripheral blood was collected from normal pregnant women at 10-14 weeks of
379 pregnancy (N=6). All tissues and peripheral blood were provided by the Research Centre

380 for Women's and Infants' Health Bio Bank program at Sinai Health System and are
381 collected following informed written consent (process n# 20-0101-E) and in adherence
382 with the policies of the Sinai Health System and the University of Toronto Research Ethics
383 Board and in accordance with the Helsinki declaration on the use of human tissues.
384

385 **Human Placental Explant Culture**

386 Second trimester human placentae (16 to 20 weeks) from the elective termination of
387 singleton pregnancies were used to set up the floating explant culture as described earlier
388 (Lye *et al.*, 2015). Briefly, placental specimens were placed into 1% phosphate-buffered
389 saline (PBS) with $Ca^{2+}$and Mg^{2+} and transported to the laboratory. Tissues were
390 dissected into villous clusters of approximately 15 to 30 mg, and three villous explants
391 were cultured per well in 12-well plates that contained Dulbec-co's modified Eagle's
392 medium/F12, Normocin antibiotic (Invivogen, San Diego, CA), and 1 insulin, transferrin,
393 and selenium-A (Invitrogen, Grand Island, NY) that was previously equilibrated at 8% O_2
394 (CO_2, 37 °C) for 24 hours. Explants were cultured for 24 hours and then randomly divided
395 into treatment groups. Explants were treated with LPS from Escherichia coli (10 µg/mL
396 L4391, Sigma-Aldrich, St. Louis, MO) or vehicle for 4 or 24 hours (Lye *et al.*, 2015).
397 Explants were then collected and stored at 80°C for total RNA.

398 **Immunohistochemistry**

399 Placental tissues (N=5/6group) were processed for immunohistochemical analysis as
400 previously described (Lye *et al.*, 2019). Briefly, slides were deparaffinized, rehydrated,
401 and subjected to heat mediated antigen retrieval with 10mM sodium citrate Ph6.0 for

402 CD206 and neutrophil primary antibodies, or 1mM EDTA Ph9.0 for MHC-II, CD68 and
403 ACE2. After blocking with Dako protein block (Dako, Mississauga, ON, Canada), the
404 slides were incubated overnight at 4°C with primary antibodies: anti-rabbit ACE2 (1:200,
405 ab15348, Abcam, Toronto, ON, Canada USA) anti-rabbit MHC-II (M1 marker) (1:400,
406 ab180779, Abcam), anti-rabbit mannose receptor (CD206 (M2),1:200, ab64693, Abcam),
407 anti-mouse CD68 (macrophage) (1:100, Dako), anti-rabbit neutrophil (NE)(1:100,
408 ab21595, abcam) was added instead of the primary antibody. After incubation, the slides
409 were washed and incubated with the corresponding biotinylated secondary antibody
410 (1:300, 1 hour, Dako). Sections were washed in 1× PBS (3 × 5 min) and incubated with
411 streptavidin-HRP (1 h; Dako); immunostaining was detected with the peroxidase
412 substrate kit DAB (Dako). The slides were counterstained with hematoxylin, dehydrated
413 in ascending concentrations of ethanol, and cover slipped with mounting medium.
414 Visualization was undertaken with an Olympus BX61 upright, motorized microscope, and
415 representative images were captured using an Olympus DP72 digital camera (Olympus,
416 Tokyo, Japan. Negative controls were performed using either isotype Mouse IgG1 or
417 rabbit IgG/IgG1 antibodies.

418 **Image Analysis and Quantification**

419 Quantification of macrophages subtypes and neutrophils in placental tissues (N=5-
420 6/group) were performed using an Olympus BX61 microscope equipped with an Olympus
421 DP72 camera, and the newCAST software (Visopharm). Counts were performed as
422 previously described (Dunk *et al.*, 2019), using a standard protocol that assigned random
423 counting frames covering 5% of each total masked tissue area. Brown, positively-staining

424 cells and blue, negatively-staining cells (haematoxylin-stained) were counted at 10X
425 magnification. A positively stained ratio was generated by dividing the total numbers of
426 brown, positively-stained cells by the total number of cells counted in the tissue area).

427

428 **Double immunofluorescence staining**

429 Different protocols were used for the simultaneous detection of two antigens depending
430 on the availability of primary antibodies raised in the same or different species. For the
431 localization of ACE2+CD68 (primary antibodies different species), immunofluorescence
432 experiments were performed as described previously (Nadeem *et al.*, 2013). In brief, ChA
433 placental tissue slides were deparaffinized, rehydrated, and subjected to heat mediated
434 antigen retrieval with 1mM EDTA Ph9. Autofluorescence was reduced using 0.1% Sudan
435 Black in 70% ethanol (1 minute) and non-specific binding was blocked using 0.1% BSA,
436 0.3% Triton X-100 and 1% donkey serum in PBS for 1 hour. Placental slides were
437 incubated with primary antibodies ACE2 (1:100, ab15348, Abcam), anti-mouse CD68
438 (1:100, Dako), anti-mouse IgG1 (Dako) and anti-rabbit Igg1 (ab171870, Abcam) added
439 as an isotype control overnight at 4°C. Subsequently, ACE2 + CD68 slides were washed
440 three times and incubated with fluorescent secondary antibodies, using either the anti-
441 mouse Alexa 488 (1:1000) or the anti-rabbit Alexa 594 (1:1000) secondary antibodies
442 (Thermo Fisher Scientific and counterstained with 1 µg/mL of DAPI, for 1 hour).

443 For the localization of ACE2+MHC-II (M1), ACE2+CD206 (M2) and ACE2+Neutrophil
444 elastase (NE) (primary antibodies the same species), immunofluorescence experiments

445 were performed as described previously (Salio *et al.*, 2005; Dunk *et al.*, 2018; Choudhury
446 *et al.*, 2019). In brief, ChA placental slides were deparaffinized, rehydrated, and subjected
447 to antigen retrieval with 1mM EDTA Ph9.0. Autofluorescence was reduced using 0.1%
448 Sudan Black in 70% ethanol (1 minutes) and non-specific binding was blocked using 0.1%
449 BSA, 0.3% Triton X-100 and 1% donkey serum in PBS for 1 hour. Placental tissues slides
450 were incubated with primary antibodies ACE2 (1:100, ab15348, Abcam) overnight at 4°C.
451 Subsequently, ACE2 slides were washed three times and incubated with fluorescent
452 secondary antibodies using anti-rabbit Alexa 594 (1:1000) (Thermo Fisher Scientific for 1
453 hour). Slides were washed three times and blocked with 0.1% BSA, 0.3% Triton X-100
454 and 5% goat serum in PBS for 1 h. Slides were incubated with primary antibodies anti
455 rabbit-MHC II (M1) (1:100, Abcam), anti-rabbit mannose receptor (CD206, M2,1:100,
456 Abcam) anti-rabbit NE (1:100, Abcam) and anti-rabbit IgG1 (Abcam) added as an isotype
457 control overnight at 4°C. Slides were incubated with the corresponding biotinylated
458 secondary antibody (1:300, 1 h, Dako) then washed three times and incubated with
459 Streptavidin-Alexa488 (1:2000, Thermo Fisher Scientific and nuclei were stained with 1
460 μg/mL of DAPI, for 1 h). All slides from the primary antibodies as the same or different
461 species were washed three times. Fluorescent microscopy was performed using a
462 spinning disc confocal microscope at various magnifications.

463 **Quantitative Real Time PCR (qPCR)**

464 Total RNA was isolated from flash frozen, stored in -80C placental specimens using
465 the RNeasy Plus Universal Mini Kit (73404, Qiagen, Toronto, ON, Canada), as previously
466 described (Lye *et al.*, 2019). RNA concentration and purity were assessed using a

467 NanoDrop1000 Spectrophotometer (Thermo Scientific). RNA was reverse transcribed
468 into cDNA using the iScript Reverse Transcription Supermix (Bio-Rad). *ACE2*, *IL-6*, *IL-8*,
469 *TNFα* and *CCL2* mRNA levels were measured by qPCR using SYBR Green reagent
470 (Sigma-Aldrich) and the CFX 380 Real-Time system C1000 TM Thermal Cycler (Bio-
471 Rad), with the following cycling conditions: initial denaturation at 95 °C (2 min) followed
472 by 39 cycles of denaturation at 95 °C (5 s) and combined annealing and extension at 60
473 °C (20 s). Gene expression was normalized to the geometric mean of selected reference
474 genes, including DNA topoisomerase 1 (*TOP1*) and the zeta polypeptide (*YWHAZ*) which
475 had stable expression across pregnancies complicated by PTB or ChA or from SVD or
476 ELCS groups. *TOP1* and TATA-box binding protein (*TBP*) were used in studies of LPS
477 treatments in second trimester explants. The relative expression of target genes was
478 calculated by the 2-ΔΔCT method (Livak & Schmittgen, 2001). The primer sequences of
479 all the assessed genes are shown in Table 2.
480

Table 2. List of primers used in this study.

Primer name	Sequence	Reference
ACE2	Forward: 5'- GGAGTGATAGTGGTTGGCATTGTC -3 Reverse: 5'-GCTAATATCGATGGAGGCATAAGGA-3'	*
IL-6	Forward: 5'-TGCAGAAAAAGGCAAAGAAT-3' Reverse: 5'-CTGACCAGAAGAAGGAATGC-3'	(Lye *et al.*, 2019)
IL-8	Forward: 5'-TGGGAACAAGAGGGCATCTG-3' Reverse: 5'-CCACCACTGCATCAAATTCATG-3'	(Lye *et al.*, 2019)
CCL2	Forward: 5'-TTCATTCCCCAAGGGCTCGCTCA -3' Reverse: 5'-AGCACAGATCTCCTTGGCCACAA -3'	(Lye *et al.*, 2015)
TNFα	Forward: 5'-CCTGGGGAACTCTTCCCTCTGGGG -3' Reverse: 5'-CAGGCGCCACCACGCTCTTC -3'	*
TBP	Forward: 5'-TGC ACA GGA GCC AAG AGT GAA -3' Reverse: 5'-CAC ATC ACA GCT CCC CAC CA -3'	(Keidar *et al.*, 2005)
YWHAZ	Forward: 5'-CCGCCAGGACAAACCAGTAT-3'	(Drewlo *et al.*, 2012)

	Reverse: 5'-CAC ATC ACA GCT CCC CAC CA-3'	
TOP1	Forward: 5'-GATGAACCTGAAGATGATGGC-3'	(Drewlo *et al.*, 2012)
	Reverse: 5'-TCAGCATCATCCTCATCTCG-3'	

*Gene specific primers were designed with Primer-BLAST (http://www.ncbi.nlm.nih.gov/tools/primer-blast).

481

482 **Immunoblotting**

483 Western blot analysis was conducted as previously described (Lye *et al.*, 2019) Briefly,
484 protein isolated from cultured cells was extracted by sonication using lysis buffer (1 mol/L
485 Tris-HCL pH 6.8, 2% SDS, 10% glycerol with added protease and phosphatase inhibitor
486 cocktail; Thermo Scientific). The protein concentration was determined with the Pierce
487 BCA Protein Assay kit (Thermo Scientific). Proteins were separated by electrophoresis
488 (30 µg 100 V, 1 h) using SDS polyacrylamide gels (8%). Proteins were then transferred
489 (10 min) to polyvinylidene fluoride (PVDF) membrane using Trans-Blot Turbo (Bio-Rad).
490 Membranes were blocked with skim milk (5%; 1 h at room temperature). The primary
491 antibodies used were anti-rabbit ACE2 (dilution 1:1000; Abcam, ab108209, Toronto, ON,
492 Canada) and anti-goat *β*-actin (dilution 1:2000; Santa Cruz Biotechnology, Dallas, TX,
493 USA). Blots were incubated with primary antibodies overnight at 4 °C. The PVDF
494 membranes were subsequently incubated for 1 h with HRP-linked anti-goat secondary
495 antibody (GE Healthcare Bio-Science, Baie d'Urfe, QC, Canada) at concentrations of
496 1:10,000. Protein-antibody complexes were detected by incubating (for 5 min) the PVDF
497 membranes with Laminate Crescendo Western HRP Substrate (Millipore, Oak Drive, CA,
498 USA) and chemiluminescence was detected under UV by using the ChemiDoc™ MP

499 Imaging system (Bio-Rad). The protein band intensity was quantified using Image Lab™
500 software.

501 **Immune cell isolation**

502 Peripheral blood samples were collected prospectively into EDTA blood collection tubes
503 from pregnant women in the first trimester (10-14 gestational weeks) during the regular
504 antenatal visit. Monocytes and lymphocytes were isolated separately using the
505 RosetteSep Human Total Lymphocyte Enrichment Cocktail and the RosetteSep Human
506 Total Lymphocyte Enrichment Cocktail (both from Stemcell Technologies, BC, CA)
507 following manufacturer's instructions as described earlier (Paquette *et al.*, 2018).
508 RosetteSep technology uses high-density gradient centrifugation to generate a highly
509 purified and stable leukocyte fraction RNA expression studies. Following isolation, the
510 monocytes and lymphocytes were re-suspended in RPMI-1640 with 10% FBS. Primary
511 human neutrophils were isolated by Histopaque double density gradient method,
512 consisting of HISTOPAQUE®-1119 and HISTOPAQUE®-1077 (Sigma-Aldrich, MO,
513 USA). Neutrophils were collected, washed twice in HBSS+ and spun again (Amsalem *et*
514 *al.*, 2014).

515 **Flow cytometry**

516 Direct immunofluorescence staining was performed using peripheral blood collected from
517 pregnant women at 10-14 weeks of pregnancy. In brief, the whole blood (50µl) was
518 stained with LIVE/DEAD® fixable cell stain kit (L/D-violet; Invitrogen) and then incubated
519 with human Fc block (BD Pharmingen) and incubated for 30 minutes. To detect the
520 expression of ACE2 protein, surface staining was conducted by Alexa Fluor® 700-

521 conjugated mouse anti-human ACE-2 (R&D Systems) and APC-H7 mouse anti-human
522 CD45 (BD Biosciences) antibodies. Cells were washed and resuspended in stabilizing
523 fixative buffer (BD Biosciences) to preserve immunofluorescence staining signals of
524 human blood.
525 Flow cytometric data were acquired with a Gallios flow cytometer (Beckman Coulter).
526 Data analyses were performed by FlowJo V10 (TreeStar) or Kaluza 2 (Beckman Coulter)
527 software. Only viable CD45+ blood cells were analyzed for their ACE2 expression.
528 Circulating lymphocytes, monocytes and granulocytes were recognized by their distinct
529 morphological features in the forward and side scatter distribution.

530 **Statistical Analysis**

531 All analyses were conducted blind to the experimental conditions. Data analyses
532 were performed with Prism version 8 (GraphPad Software Inc., San Diego, CA, USA)
533 qPCR data were assessed for normal distribution using D'Agostino and Pearson or the
534 Shapiro-Wilk test; outliers were identified using "QuickCalcs" Outlier calculator program
535 (version 7.0; GraphPad Software, Inc., San Diego, CA). Gene and protein expression,
536 number of macrophages, and maternal immune cell were analyzed using one-way
537 ANOVA followed by Tukey's multiple comparisons test. Results from LPS-treated
538 explants were assessed by paired *t*-test. Gene expression of the LPS treated explants
539 were normalized to their respected vehicle group at both 4 and 24 hours. Differences
540 were considered statistically significant when $p < 0.05$.

541

542

543 **Author Contributions**

544 Conceptualization: PL, CED, SGM, SJL; Funding acquisition: SJL, SGM;

545 Methodology: PL, CED, JZ, JN, GEI, SL; Project administration SGM, SJL; Supervision:
546 SGM, SJL; Validation: PL, CED, JZ; Writing - original draft: PL, CED, HH, EB, JZ, YW;
547 Writing - review & editing: CED, PL, HH, JN, YW, GEI, EB, SGM, SJL.

548

549 **Acknowledgement**

550 The authors thank the donors, RCWIH BioBank, the Lunenfeld-Tanenbaum Research
551 Institute, and the Mount Sinai Hospital/UHN Department of Obstetrics and Gynaecology
552 for the human specimens used in this study (http://biobank.lunenfeld.ca). We are grateful
553 for the assistance provided by Mrs. Anna Dorogin in optimising immunostaining, Mrs.
554 Elzbieta Matysiak-Zablocki with the isolation of granulocytes, monocytes and
555 lymphocytes and Dr. Oksana Shynlova with the isolation of maternal immune cell
556 protocols.

557 **Additional Information**

558 The authors report no conflict of interest.

559 E.B. is supported by the Coordenaçao de Aperfeiçoamento Pessoal de Nível Superior
560 [CAPES]; finance code 001, CAPES-Print fellowship). S.J.L. is supported by a grant
561 (FDN-143262) from the Canadian Institutes of Health Research (CIHR). S.G.M. is
562 supported by a grant (FDN-148368) from the CIHR.

The funders had no role in the experimental design, data acquisition, analysis, and interpretation or in the manuscript writing and conception of this study. The corresponding authors had full access to all the data in the study and had final responsibility for the decision to submit for publication.

Additional Information

Available from the authors upon reasonable request

References

Algarroba, G.N., Rekawek, P., Vahanian, S.A., Khullar, P., Palaia, T., Peltier, M.R., Chavez, M.R. & Vintzileos, A.M. (2020) Visualization of SARS-CoV-2 virus invading the human placenta using electron microscopy. *American journal of obstetrics and gynecology*.

Amsalem, H., Kwan, M., Hazan, A., Zhang, J., Jones, R.L., Whittle, W., Kingdom, J.C., Croy, B.A., Lye, S.J. & Dunk, C.E. (2014) Identification of a novel neutrophil population: proangiogenic granulocytes in second-trimester human decidua. *Journal of immunology (Baltimore, Md. : 1950)*, **193**, 3070-3079.

Baud, D., Greub, G., Favre, G., Gengler, C., Jaton, K., Dubruc, E. & Pomar, L. (2020) Second-Trimester Miscarriage in a Pregnant Woman With SARS-CoV-2 Infection. *Jama*, **323**, 2198-2200.

Bloise, E., Zhang, J., Nakpu, J., Hamada, H., Dunk, C.E., Li, S., Imperio, G.E., Nadeem, L., Kibschull, M., Lye, P., Matthews, S.G. & Lye, S.J. (2020) Expression of severe acute respiratory syndrome coronavirus 2 cell entry genes, angiotensin-converting enzyme 2 and transmembrane protease serine 2, in the placenta across gestation and at the maternal-fetal interface in pregnancies complicated by preterm birth or preeclampsia. *American journal of obstetrics and gynecology*. S0002-9378(20)30884-X.

Blumberg, D.A., Underwood, M.A., Hedriana, H.L. & Lakshminrusimha, S. (2020) Vertical Transmission of SARS-CoV-2: What is the Optimal Definition? *American journal of perinatology*, **37**, 769-772.

597 Capobianco, G., Saderi, L., Aliberti, S., Mondoni, M., Piana, A., Dessole, F., Dessole, M.,
598 Cherchi, P.L., Dessole, S. & Sotgiu, G. (2020) COVID-19 in pregnant women: A
599 systematic review and meta-analysis. *European journal of obstetrics, gynecology, and*
600 *reproductive biology*, **252**, 543-558.
601
602 Cappelletti, M., Presicce, P. & Kallapur, S.G. (2020) Immunobiology of Acute
603 Chorioamnionitis. *Front Immunol*, **11**, 649-649.
604
605 Cardenas, I., Mor, G., Aldo, P., Lang, S.M., Stabach, P., Sharp, A., Romero, R., Mazaki-Tovi, S.,
606 Gervasi, M. & Means, R.E. (2011) Placental viral infection sensitizes to endotoxin-
607 induced pre-term labor: a double hit hypothesis. *American journal of reproductive*
608 *immunology (New York, N.Y. : 1989)*, **65**, 110-117.
609
610 Chen, H., Guo, J., Wang, C., Luo, F., Yu, X., Zhang, W., Li, J., Zhao, D., Xu, D., Gong, Q.,
611 Liao, J., Yang, H., Hou, W. & Zhang, Y. (2020) Clinical characteristics and intrauterine
612 vertical transmission potential of COVID-19 infection in nine pregnant women: a
613 retrospective review of medical records. *Lancet (London, England)*, **395**, 809-815.
614
615 Choudhury, R.H., Dunk, C.E., Lye, S.J., Harris, L.K., Aplin, J.D. & Jones, R.L. (2019) Decidual
616 leucocytes infiltrating human spiral arterioles are rich source of matrix metalloproteinases
617 and degrade extracellular matrix in vitro and in situ. *American journal of reproductive*
618 *immunology (New York, N.Y. : 1989)*, **81**, e13054.
619
620 Crackower, M., Sarao, R., Oudit, G., Yagil, C., Kozieradzki, I., Scanga, S., Oliveira-dos-Santos,
621 A., Costa, J., Zhang, L., Pei, Y., Scholey, J., Ferrario, C., Manoukian, A., Chappell, M.,
622 Backx, P., Yagil, Y. & Penninger, J. (2002) Angiotensin-converting enzyme 2 is an
623 essential regulator of heart function. *Nature*, **417**, 822-828.
624
625 Dong, L., Tian, J., He, S., Zhu, C., Wang, J., Liu, C. & Yang, J. (2020) Possible Vertical
626 Transmission of SARS-CoV-2 From an Infected Mother to Her Newborn. *Jama*, **323**,
627 1846-1848.
628
629 Drewlo, S., Levytska, K. & Kingdom, J. (2012) Revisiting the housekeeping genes of human
630 placental development and insufficiency syndromes. *Placenta*, **33**, 952-954.
631
632 Dunk, C., Kwan, M., Hazan, A., Walker, S., Wright, J.K., Harris, L.K., Jones, R.L., Keating, S.,
633 Kingdom, J.C.P., Whittle, W., Maxwell, C. & Lye, S.J. (2019) Failure of Decidualization
634 and Maternal Immune Tolerance Underlies Uterovascular Resistance in Intra Uterine
635 Growth Restriction. *Frontiers in Endocrinology*, **10**.
636
637 Dunk, C.E., Pappas, J.J., Lye, P., Kibschull, M., Javam, M., Bloise, E., Lye, S.J., Szyf, M. &
638 Matthews, S.G. (2018) P-Glycoprotein (P-gp)/ABCB1 plays a functional role in
639 extravillous trophoblast (EVT) invasion and is decreased in the pre-eclamptic placenta.
640 *Journal of cellular and molecular medicine*, **22**, 5378-5393.
641

642 Facchetti, F., Bugatti, M., Drera, E., Tripodo, C., Sartori, E., Cancila, V., Papaccio, M.,
643 Castellani, R., Casola, S., Boniotti, M.B., Cavadini, P. & Lavazza, A. (2020) SARS-
644 CoV2 vertical transmission with adverse effects on the newborn revealed through
645 integrated immunohistochemical, electron microscopy and molecular analyses of
646 Placenta. *EBioMedicine*, **59**, 102951.
647
648 Francis, F., Bhat, V., Mondal, N., Adhisivam, B., Jacob, S., Dorairajan, G. & Harish, B.N.
649 (2019) Fetal inflammatory response syndrome (FIRS) and outcome of preterm neonates -
650 a prospective analytical study. *The journal of maternal-fetal & neonatal medicine : the*
651 *official journal of the European Association of Perinatal Medicine, the Federation of*
652 *Asia and Oceania Perinatal Societies, the International Society of Perinatal Obstet*, **32**,
653 488-492.
654
655 Glauser, M.P., Zanetti, G., Baumgartner, J.D. & Cohen, J. (1991) Septic shock: pathogenesis.
656 *Lancet (London, England)*, **338**, 732-736.
657
658 Gomez-Lopez, N., Romero, R., Maymon, E., Kusanovic, J.P., Panaitescu, B., Miller, D., Pacora,
659 P., Tarca, A.L., Motomura, K., Erez, O., Jung, E., Hassan, S.S. & Hsu, C.D. (2019)
660 Clinical chorioamnionitis at term IX: in vivo evidence of intra-amniotic inflammasome
661 activation. *Journal of perinatal medicine*, **47**, 276-287.
662
663 Gomez-Lopez, N., Romero, R., Xu, Y., Leng, Y., Garcia-Flores, V., Miller, D., Jacques, S.M.,
664 Hassan, S.S., Faro, J., Alsamsam, A., Alhousseini, A., Gomez-Roberts, H., Panaitescu,
665 B., Yeo, L. & Maymon, E. (2017) Are amniotic fluid neutrophils in women with
666 intraamniotic infection and/or inflammation of fetal or maternal origin? *American journal*
667 *of obstetrics and gynecology*, **217**, 693.e691-693.e616.
668
669 Hamilton, S., Oomomian, Y., Stephen, G., Shynlova, O., Tower, C.L., Garrod, A., Lye, S.J. &
670 Jones, R.L. (2012) Macrophages infiltrate the human and rat decidua during term and
671 preterm labor: evidence that decidual inflammation precedes labor. *Biology of*
672 *reproduction*, **86**, 39.
673
674 Hamming, I., Timens, W., Bulthuis, M.L.C., Lely, A.T., Navis, G.J. & van Goor, H. (2004)
675 Tissue distribution of ACE2 protein, the functional receptor for SARS coronavirus. A
676 first step in understanding SARS pathogenesis. *J Pathol*, **203**, 631-637.
677
678 Jia, H.P., Look, D.C., Shi, L., Hickey, M., Pewe, L., Netland, J., Farzan, M., Wohlford-Lenane,
679 C., Perlman, S. & McCray, P.B., Jr. (2005) ACE2 receptor expression and severe acute
680 respiratory syndrome coronavirus infection depend on differentiation of human airway
681 epithelia. *J Virol*, **79**, 14614-14621.
682
683 Karimi-Zarchi, M., Neamatzadeh, H., Dastgheib, S.A., Abbasi, H., Mirjalili, S.R., Behforouz, A.,
684 Ferdosian, F. & Bahrami, R. (2020) Vertical Transmission of Coronavirus Disease 19
685 (COVID-19) from Infected Pregnant Mothers to Neonates: A Review. *Fetal and*
686 *pediatric pathology*, **39**, 246-250.
687

688 Keidar, S., Gamliel-Lazarovich, A., Kaplan, M., Pavlotzky, E., Hamoud, S., Hayek, T., Karry, R.
689 & Abassi, Z. (2005) Mineralocorticoid receptor blocker increases angiotensin-converting
690 enzyme 2 activity in congestive heart failure patients. *Circulation research*, **97**, 946-953.
691
692 Kim, C.J., Romero, R., Chaemsaithong, P., Chaiyasit, N., Yoon, B.H. & Kim, Y.M. (2015)
693 Acute chorioamnionitis and funisitis: definition, pathologic features, and clinical
694 significance. *American journal of obstetrics and gynecology*, **213**, S29-52.
695
696 Knöfler, M., Haider, S., Saleh, L., Pollheimer, J., Gamage, T. & James, J. (2019) Human
697 placenta and trophoblast development: key molecular mechanisms and model systems.
698 *Cellular and molecular life sciences : CMLS*, **76**, 3479-3496.
699
700 Kwon, J.Y., Romero, R. & Mor, G. (2014) New insights into the relationship between viral
701 infection and pregnancy complications. *American journal of reproductive immunology*
702 *(New York, N.Y. : 1989)*, **71**, 387-390.
703
704 Li, F. (2016) Structure, Function, and Evolution of Coronavirus Spike Proteins. *Annual review of*
705 *virology*, **3**, 237-261.
706
707 Li, G., He, X., Zhang, L., Ran, Q., Wang, J., Xiong, A., Wu, D., Chen, F., Sun, J. & Chang, C.
708 (2020a) Assessing ACE2 expression patterns in lung tissues in the pathogenesis of
709 COVID-19. *J Autoimmun*, **112**, 102463-102463.
710
711 Li, M., Chen, L., Zhang, J., Xiong, C. & Li, X. (2020b) The SARS-CoV-2 receptor ACE2
712 expression of maternal-fetal interface and fetal organs by single-cell transcriptome study.
713 *PloS one*, **15**, e0230295.
714
715 Liu, X., Yin, S., Chen, Y., Wu, Y., Zheng, W., Dong, H., Bai, Y., Qin, Y., Li, J., Feng, S. &
716 Zhao, P. (2018) LPS-induced proinflammatory cytokine expression in human airway
717 epithelial cells and macrophages via NF-κB, STAT3 or AP-1 activation. *Molecular*
718 *medicine reports*, **17**, 5484-5491.
719
720 Livak, K.J. & Schmittgen, T.D. (2001) Analysis of relative gene expression data using real-time
721 quantitative PCR and the 2(-Delta Delta C(T)) Method. *Methods (San Diego, Calif.)*, **25**,
722 402-408.
723
724 Lye, P., Bloise, E., Javam, M., Gibb, W., Lye, S.J. & Matthews, S.G. (2015) Impact of bacterial
725 and viral challenge on multidrug resistance in first- and third-trimester human placenta.
726 *The American journal of pathology*, **185**, 1666-1675.
727
728 Lye, P., Bloise, E., Nadeem, L., Peng, C., Gibb, W., Ortiga-Carvalho, T.M., Lye, S.J. &
729 Matthews, S.G. (2019) Breast Cancer Resistance Protein (BCRP/ABCG2) Inhibits Extra
730 Villous Trophoblast Migration: The Impact of Bacterial and Viral Infection. *Cells*, **8**.
731

732 Nadeem, L., Brkic, J., Chen, Y.F., Bui, T., Munir, S. & Peng, C. (2013) Cytoplasmic
733 mislocalization of p27 and CDK2 mediates the anti-migratory and anti-proliferative
734 effects of Nodal in human trophoblast cells. *Journal of cell science*, **126**, 445-453.
735
736 Paquette, A.G., Shynlova, O., Kibschull, M., Price, N.D. & Lye, S.J. (2018) Comparative
737 analysis of gene expression in maternal peripheral blood and monocytes during
738 spontaneous preterm labor. *American journal of obstetrics and gynecology*, **218**,
739 345.e341-345.e330.
740
741 Pringle, K., Tadros, M., Callister, R.J. & Lumbers, E. (2011a) The expression and localization of
742 the human placental prorenin/renin-angiotensin system throughout pregnancy: Roles in
743 trophoblast invasion and angiogenesis? *Placenta*, **32**, 956-962.
744
745 Pringle, K.G., Tadros, M.A., Callister, R.J. & Lumbers, E.R. (2011b) The expression and
746 localization of the human placental prorenin/renin-angiotensin system throughout
747 pregnancy: roles in trophoblast invasion and angiogenesis? *Placenta*, **32**, 956-962.
748
749 Qiao, J. (2020) What are the risks of COVID-19 infection in pregnant women? *Lancet (London,*
750 *England)*, **395**, 760-762.
751
752 Rasmussen, S.A., Smulian, J.C., Lednicky, J.A., Wen, T.S. & Jamieson, D.J. (2020) Coronavirus
753 Disease 2019 (COVID-19) and pregnancy: what obstetricians need to know. *American*
754 *journal of obstetrics and gynecology*, **222**, 415-426.
755
756 Redline, R.W., Faye-Petersen, O., Heller, D., Qureshi, F., Savell, V. & Vogler, C. (2003)
757 Amniotic infection syndrome: nosology and reproducibility of placental reaction patterns.
758 *Pediatric and developmental pathology : the official journal of the Society for Pediatric*
759 *Pathology and the Paediatric Pathology Society*, **6**, 435-448.
760
761 Romero, R., Salafia, C.M., Athanassiadis, A.P., Hanaoka, S., Mazor, M., Sepulveda, W. &
762 Bracken, M.B. (1992) The relationship between acute inflammatory lesions of the
763 preterm placenta and amniotic fluid microbiology. *American journal of obstetrics and*
764 *gynecology*, **166**, 1382-1388.
765
766 Salio, C., Lossi, L., Ferrini, F. & Merighi, A. (2005) Ultrastructural evidence for a pre- and
767 postsynaptic localization of full-length trkB receptors in substantia gelatinosa (lamina II)
768 of rat and mouse spinal cord. *The European journal of neuroscience*, **22**, 1951-1966.
769
770 Schwartz, D.A. (2020) An Analysis of 38 Pregnant Women with COVID-19, Their Newborn
771 Infants, and Maternal-Fetal Transmission of SARS-CoV-2: Maternal Coronavirus
772 Infections and Pregnancy Outcomes. *Archives of pathology & laboratory medicine*.
773
774 Shah, P.S., Diambomba, Y., Acharya, G., Morris, S.K. & Bitnun, A. (2020) Classification
775 system and case definition for SARS-CoV-2 infection in pregnant women, fetuses, and
776 neonates. *Acta obstetricia et gynecologica Scandinavica*, **99**, 565-568.
777

Shynlova, O., Nadeem, L., Zhang, J., Dunk, C. & Lye, S. (2020) Myometrial activation: Novel concepts underlying labor. *Placenta*, **92**, 28-36.

Silasi, M., Cardenas, I., Kwon, J.Y., Racicot, K., Aldo, P. & Mor, G. (2015) Viral infections during pregnancy. *American journal of reproductive immunology (New York, N.Y. : 1989)*, **73**, 199-213.

Valdés, G., Neves, L.A., Anton, L., Corthorn, J., Chacón, C., Germain, A.M., Merrill, D.C., Ferrario, C.M., Sarao, R., Penninger, J. & Brosnihan, K.B. (2006) Distribution of angiotensin-(1-7) and ACE2 in human placentas of normal and pathological pregnancies. *Placenta*, **27**, 200-207.

Vickers, C., Hales, P., Kaushik, V., Dick, L., Gavin, J., Tang, J., Godbout, K., Parsons, T., Baronas, E., Hsieh, F., Acton, S., Patane, M., Nichols, A. & Tummino, P. (2002) Hydrolysis of biological peptides by human angiotensin-converting enzyme-related carboxypeptidase. *The Journal of biological chemistry*, **277**, 14838-14843.

Wan, Y., Shang, J., Graham, R., Baric, R.S. & Li, F. (2020) Receptor Recognition by the Novel Coronavirus from Wuhan: an Analysis Based on Decade-Long Structural Studies of SARS Coronavirus. *Journal of Virology*, **94**, e00127-00120.

Wang, S., Guo, L., Chen, L., Liu, W., Cao, Y., Zhang, J. & Feng, L. (2020) A Case Report of Neonatal 2019 Coronavirus Disease in China. *Clinical Infectious Diseases*.

Zamaniyan, M., Ebadi, A., Aghajanpoor, S., Rahmani, Z., Haghshenas, M. & Azizi, S. (2020) Preterm delivery, maternal death, and vertical transmission in a pregnant woman with COVID-19 infection. *Prenatal diagnosis*.

Zeng, H., Xu, C., Fan, J., Tang, Y., Deng, Q., Zhang, W. & Long, X. (2020) Antibodies in Infants Born to Mothers With COVID-19 Pneumonia. *Jama*, **323**, 1848-1849.

Zhang, H., Penninger, J.M., Li, Y., Zhong, N. & Slutsky, A.S. (2020a) Angiotensin-converting enzyme 2 (ACE2) as a SARS-CoV-2 receptor: molecular mechanisms and potential therapeutic target. *Intensive Care Med*, **46**, 586-590.

Zhang, L., Jiang, Y., Wei, M., Cheng, B.H., Zhou, X.C., Li, J., Tian, J.H., Dong, L. & Hu, R.H. (2020b) [Analysis of the pregnancy outcomes in pregnant women with COVID-19 in Hubei Province]. *Zhonghua fu chan ke za zhi*, **55**, 166-171.